Host and ϕX 174 Mutations Affecting the Morphogenesis or Stabilization of the 50S Complex, a Single-Stranded DNA Synthesizing Intermediate

Martina C. Ekechukwu, D. Jason Oberste and Bentley A. Fane

Department of Biological Sciences, University of Arkansas, Fayetteville, Arkansas 72701

Manuscript received January 3, 1995
Accepted for publication May 1, 1995

ABSTRACT

The morphogenetic pathway of bacteriophage ϕX 174 was investigated in *rep* mutant hosts that specifically block stage III single-stranded DNA synthesis. The defects conferred by the mutant *rep* protein most likely affect the formation or stabilization of the 50S complex, a single-stranded DNA synthesizing intermediate, which consists of a viral prohead and a DNA replicating intermediate (preinitiation complex). ϕX 174 mutants, *ogr(rep)*, which restore the ability to propagate in the mutant *rep* hosts, were isolated. The *ogr(rep)* mutations confer amino acid substitutions in the viral coat protein, a constituent of the prohead, and the viral *A* protein, a constituent of the preinitiation complex. Four of the six coat protein substitutions are localized on or near the twofold axis of symmetry in the atomic structure of the mature virion.

BACTERIOPHAGE ϕX 174 is a small icosahedral virus of the class Microviridae. The mature virion contains 60 copies of gpF, the major coat protein, gpG, the major spike protein, 12 copies of gpH, the minor spike protein and a single-stranded (+) DNA genome complexed with 60 copies of gpJ, the DNA binding protein. The atomic structure of the mature virion is known (McKENNA *et al.* 1992, 1994). This, combined with well defined genetics and biochemistry, creates an ideal system in which to investigate icosahedral virion morphogenesis.

The morphogenetic pathway is presented in Figure 1. A comprehensive review of this material can be found in HAYASHI *et al.* (1988). Initially morphogenesis proceeds via two independent pathways, prohead assembly and DNA synthesis, through the formation of the preinitiation complex (stages I and II). The preinitiation complex consists of RFII DNA, viral gpA, viral gpC and the host cell *rep* protein or DNA helicase (AOYAMA *et al.* 1983; AOYAMA and HAYASHI 1986). The two pathways converge with the formation of the 50S complex, in which single-stranded DNA is synthesized (stage III) and concurrently packaged into the prohead (FUJISAWA and HAYASHI 1976).

The host cell *rep* protein is required for both stage II and stage III DNA synthesis (DENHARDT *et al.* 1967; FRANCKE and RAY 1971a; TESSMAN and PETERSON 1978). TESSMAN and PETERSON (1978), however, isolated *Escherichia coli rep* mutants (gro87 and gro89) that exclusively inhibited stage III DNA synthesis. In deproteinized samples of infected *rep* mutant cells, TESSMAN and PETERSON detected no single-stranded DNA. Protein containing assembly intermediates, such as the 50S complex, were not examined. There are several blocks in the assembly pathway that could result in an inhibition of single-stranded DNA synthesis: the 50S complex may not assemble due to either a block in prohead morphogenesis or preinitiation complex formation, assembled proheads and preinitiation complexes may be unable to associate, and association may lead to a nonfunctional 50S complex.

To distinguish between these alternatives, DNA and protein assembly intermediates synthesized in gro89 infected cells were examined. The results of these experiments suggest that stable 50S complexes do not assemble in gro89 infected cells. Prohead morphogenesis, however, is not inhibited. A second-site genetic analysis identified several mutations within the major coat protein, *ogr(rep)* mutations, which restore the ability of ϕX 174 to propagate in gro89 cells. Functional preinitiation complexes can form *in vitro* in the absence of the viral coat protein (AOYAMA *et al.* 1983; AOYAMA and HAYASHI 1986). Since single amino acid substitutions in the viral coat protein are enough to confer a viable phenotype in the gro89 host, the mutant *rep* proteins probably do not inhibit the formation of the preinitiation complex. Hence, the defect conferred by the mutant *rep* protein is most likely the stable association of proheads and preinitiation complexes. The clustering of the *ogr(rep)* substitutions within the atomic structure suggests that the twofold axis of symmetry (McKENNA *et al.* 1994) may play a critical role in 50S complex morphogenesis.

MATERIALS AND METHODS

Bacterial strains: The *E. coli* C strains used in this study; gro$^+$, gro87 and gro89; are described by TESSMAN and PETERSON (1976).

Corresponding author: Bentley A. Fane, Department of Biological Sciences, 629 SCEN, University of Arkansas, Fayetteville, AR 72701. E-mail: bfane@uafsysb.uark.edu

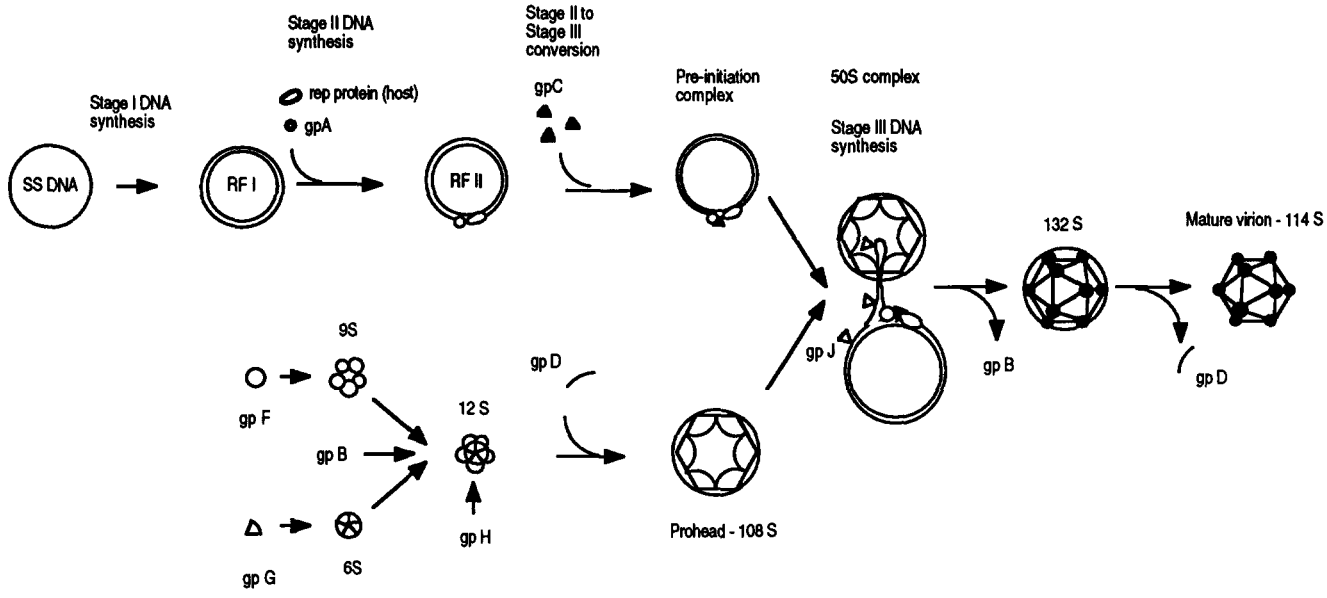

FIGURE 1.—The ϕ X174 morphogenetic pathway.

Isolation of *ogr(rep)* mutants: The *ogr(rep)* mutants were isolated by plating 10^5–10^7 plaque-forming units (pfu) on the gro87 or gro89 host. After a 5-hr incubation at 33°, revertant plaques were stabbed into indicator lawns seeded with either the gro87, gro89, or the gro$^+$ host. Gro87, gro89 and gro$^+$ plates were incubated at 33°, and an additional gro$^+$ plate was incubated at 42°. Putative *ogr(rep)* mutants were identified as those phage that could propagate on the gro87 or gro89 hosts. Temperature-sensitive mutants were identified as those which failed to grow at 42° on the gro$^+$ host.

Phage plating, stock preparation, DNA isolation, DNA sequencing, media: Detailed protocols are described in FANE and HAYASHI (1991).

Burst size experiments: The protocols for these experiments are identical to those described in FANE and HAYASHI (1991) with the exception that phage were preabsorbed to cells in HFB buffer (FANE and HAYASHI 1991) with 10 mM $MgCl_2$ and 5.0 mM $CaCl_2$ for 12 min at 37°. The adsorption mixtures were then spun in a microcentrifuge for 5.0 min. The supernatants were removed and the cell pellets were resuspended in TK (tryptone-KCl) broth with 10 mM $MgCl_2$ and 5 mM $CaCl_2$. The level of unabsorbed phage was determined by titering both the resuspended pellet before further incubation and the supernatant. Infections were then handled as previously described.

Mutagenic oligonucleotide rescue experiments: The *in vitro* DNA synthesis and transformation protocols are described in FANE *et al.* (1993). Mutagenic oligonucleotides were purchased from Genostys Biotechnologies Inc., and designed to introduce the *ogr(rep)* mutations into a wild-type background. Gro$^+$ cells were transformed with the *in vitro* DNA synthesis reactions and incubated at 33°. After 5 hr, plaques were stabbed into two indicator lawns seeded with either the gro$^+$ or gro89 host. Rescue was defined as the ability to propagate on the gro89 host. As a control, a nonmutagenic primer, which annealed to the site of one of the *ogr(rep)* mutations, was used. When a mutagenic primer was used, 100 plaques were assayed. Two hundred plaques were assayed in the experiment with the nonmutagenic primer.

Preparation of radioactive lysates and sucrose gradient centrifugation: Lysates were prepared as described in FANE *et al.* (1992). Cells were infected at an moi of 5.0 with ϕX 174 *am(E)W4* to prevent cell lysis, and incubated at 37°. At t = 11, infections were pulsed with ^{3}H thymidine or ^{3}H leucine (20 mCi/ml) and chased at t = 40 with cold thymidine or leucine (200 μg/ml). Cells were harvested at t = 60 as previously described. Sucrose gradients (5–30%, 5.0 ml) were made with a Gradient Master purchased from Biocomp Inc., following the manufacturers' instructions. Centrifugation was performed in an SW50.1 rotor at 4°. To examine larger particles (≥70S), gradients were spun for 60 min at 45,000 rpm. To examine smaller particles (≤50S), gradients were spun for 16 hr at 34,000 rpm. Gradients were fractionated and TCA precipitable counts determined as previously described.

RESULTS

Characterization of the ϕX 174 assembly pathway in gro 89 cells: Earlier experiments conducted with the *E. coli rep* mutant gro89 (TESSMAN and PETERSON 1976), are described in the Introduction. To further investigate the nature of the assembly defect conferred by the mutant *rep* protein in the gro89 host, radio-labeled DNA and protein extracts were prepared from gro89 and gro$^+$ infected cells and analyzed by sucrose gradient sedimentation as described in MATERIALS AND METHODS. The sedimentation profiles of these experiments are depicted in Figure 2.

In extracts prepared from infected gro$^+$ cells, radiolabeled proteins sediment at both 132S and 114S, the positions of the penultimate infectious intermediate and the mature virion, respectively (Figure 2). The particles in these peaks are infectious with specific infectivities of 9.0×10^4 pfu/cpm (132S) and 6.0×10^4 pfu/cpm (114S). In the extracts prepared from the gro89 infected host, however, radioactive particles sediment at 108S, the position of the prohead. The particles in this peak are not infectious (specific infectivity of 4.0×10^2 pfu/cpm). To control for possible differences between gradients, an extract of the *am(E)W4* infected gro89 cells was mixed with cold wild-type ϕX 174 marker

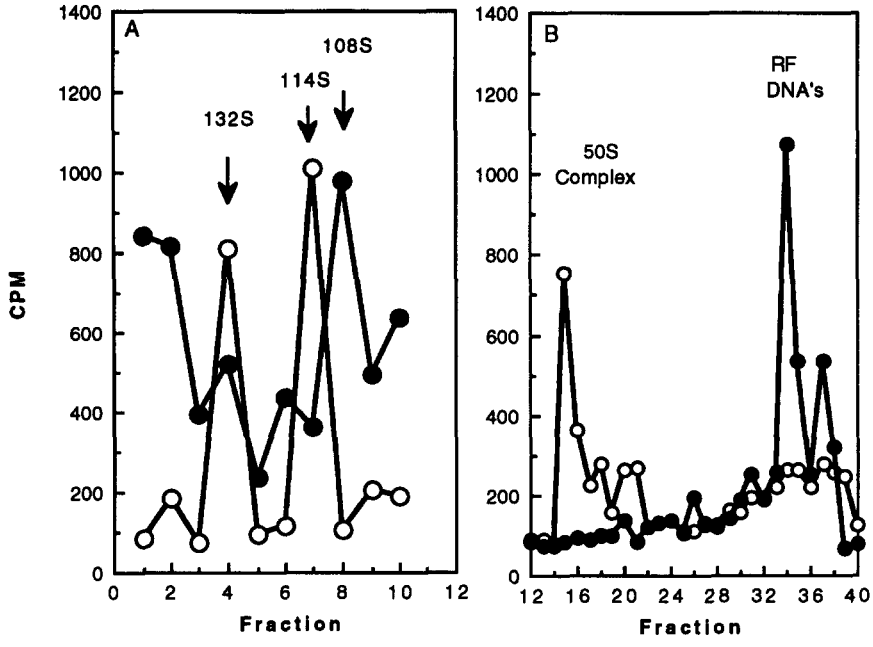

FIGURE 2.—(A) ^{3}H-protein sedimentation profiles of ϕX 174 infected cells. (B) ^{3}H-DNA sedimentation profiles of ϕX 174 infect cells. The sedimentation profile of infected gro$^+$ cell extracts is depicted (○) as is the sedimentation profile of infected gro89 cell extracts (●). Mature virions sediment at 114S. Proheads sediment at 108S. The 132S particle is an infectious intermediate. Protocols are described in MATERIALS AND METHODS.

phage in a separate experiment. The fractions were then titered on a *sup*° host. The marker phage sedimented to the left of the radioactive peak (data not shown). The results indicate that viral proheads accumulate in gro89 infected cells.

The radio-labeled DNA extracts were examined for the presence of the 50S complex and replicative form (RF) DNAs (Figure 2). In extracts of gro$^+$ infected cells, radioactive counts sediment at 50S. In extracts of gro89 infected cells, on the other hand, radioactive counts were not observed to sediment in this region. Instead, counts sediment at 20S and 30S, the positions of the RF intermediates. Sedimentation profiles generated from radio-labeled DNA extracts of gro89 infected cells, furthermore, contained no radioactive counts in the 108S-114S region (data not shown). The results of the sedimentation analyses indicate that the primary defect conferred by the mutant gro89 *rep* protein is the formation or stabilization of the 50S complex.

Isolation of ϕX 174 mutants-*ogr(rep)*: Mutant phage—*ogr(rep)*—able to propagate in the gro87 and gro89 hosts were selected as described in MATERIALS AND METHODS. The frequencies of recovery on the gro87 and gro89 hosts were 10^{-7} and 10^{-4}, respectively. To screen for the existence of secondary *ts* phenotypes, the putative *ogr(rep)* mutants were assayed for their ability to grow at 42° on the gro$^+$ (wild-type) host (Table 2). Of the 75 putative isolates, 10 displayed strong secondary phenotypes on the wild-type host. The secondary *ts* phenotype was used to map the *ogr(rep)* mutations by spot-test complementation. The results of these assays suggested that the *ts ogr(rep)* mutations resided in gene *F*, which encodes the viral coat protein. Fifteen mutants were selected for further study.

The DNA of the all *ogr(rep)* mutants was sequenced in the regions of gene *F* (coat protein) and gene *A* (DNA replication protein). Nucleotide substitutions were found in gene *F* in all of the mutants that displayed a secondary *ts* phenotype. No changes in gene *F* were found in *ogr(rep)* mutants that did not display a secondary *ts* phenotype. Substitutions, however, were found in gene *A*. The nucleotide mutations and the amino acid substitutions conferred by these mutations are listed in Table 1. Of the 15 mutants analyzed, six different mutations were found in gene *F*, and two different mutations were recovered in gene *A*. In addition, one *A/F* and one *A/A* double mutant were recovered. Several of these mutations confer changes at or to proline residues.

Oligonucleotide rescue experiments were performed to confirm the results of the DNA sequence analysis. Mutagenic primers were designed to introduce the *ogr(rep)* mutations into wild-type ϕX 174 DNA. The rescue frequency, percentage of *ogr(rep)* progeny, by the mutagenic *ogr(rep)-F P417S, A346F, S227P, S221L* and *P174R* primers were 33, 31, 14, 18 and 8%, respectively. The rescue frequency by a nonmutagenic oligonucleotide was only 0.5%.

One of the *ogr(rep)-F* mutants, *ogr(rep)-F S227P*, was previously isolated as a suppressor of cold-sensitive (cs) scaffolding proteins (Fane *et al.* 1993), or an *suD* mutation. To determine if the *ogr(rep)* and *suD* phenotypes were related, oligonucleotide rescue experiments were also performed with *cs(D)* DNA. Although the mutagenic oligonucleotides were able to introduce the *ogr(rep)* phenotype into the *cs(D)* background, none of the isolated *ogr(rep)-F/cs(D)* mutants were able to propagate at 24°, indicating that the other *ogr(rep)-F* mutations do not confer the *suD* phenotype. In addition, the previously isolated *suD* mutations were assayed

TABLE 1

Amino acids changes conferred by the *ogr(rep)* mutations

Mutation	Location and substitution[a]		Host of isolation	Number of isolates
ogr(rep)-F G88V	F88	gly → val	gro89	1
ogr(rep)-F P174R	F174	pro → arg	gro89	1
ogr(rep)-F S221L	F221	ser → leu	gro89	1
ogr(rep)-F S227P	F227	ser → pro	gro89	2
ogr(rep)-F A346V	F346	ala → val	gro89	1
ogr(rep)-F P417S	F417	pro → ser	gro89	4
ogr(rep)-A A80P	A80	ala → pro	gro89	1
ogr(rep)-A D82G	A82	asp → gly	gro89	2
ogr(rep)-A/A S59F/D82G	A59	ser → phe	gro87	1
	A82	asp → gly		
ogr(rep)-F/A S221L/A80P	F221	ser → leu	gro87	1
	A80	ala → pro		

[a] The ϕX174 sequence was originally determined by SANGER *et al.* (1978). Capital letters indicate the affected protein, numbers indicate the amino acid. Amino acid numbering for the F protein commences with serine 1 as in MCKENNA *et al.* 1992.

for the ability to propagate in the gro89 host. The *suD* mutations were unable to propagate in this host. The serine → proline substitution at amino acid 227 appears to be unique in conferring both *suD* and *ogr(rep)* phenotypes.

Characterization of the *ogr(rep)* mutants: The eop's (efficiency of plating) of the *ogr(rep)* mutations are displayed in Table 2. The *ogr(rep)-F* mutations only restore growth in the gro89 host. Although the mutants plate with relatively high efficiencies, plaque morphologies of some of these mutants, most notably *ogr(rep)-F S221L* and *ogr(rep)-F S227P*, are characteristically small. In addition, gene *F* mutants display a strong secondary *ts* phenotype in either the gro$^+$ or gro89 hosts at elevated temperatures ($\geq$37°). In many cases the *ts* phenotype has a host range component. The *ogr(rep)-F S227P* mutant, for example, is permissive for growth in the gro89 host at 42°, but restrictive in the gro$^+$ host. This suggests that the secondary *ts* phenotypes reflect defects in assembly or function. If the *ts* defect affected protein folding, for example, it is reasonable to assume that the mutant would not exhibit this host range phenomenon, but display the same *ts* phenotype in all hosts. The isolated *ogr(rep)* mutants do not propagate in an *E. coli* C strain containing the *rep3* allele (data not shown). The *rep3* allele (DENHARDT *et al.* 1967) blocks ϕX 174 stage II DNA synthesis, an earlier point in the pathway than 50S complex formation, and most likely represents a null allele of this gene.

Only one single mutant, *ogr(rep)-A A80P*, restores growth in the gro87 host. While the *ogr(rep)-A/A S59F/D82G* double mutant propagates in the gro 87 host, the *ogr(rep)-A D82G* single mutant does not. The two mutations in the *ogr(rep)-A/A S59F/D82G* were sepa-

TABLE 2

Efficiency of plating of *ogr(rep)* mutants

	33°			37°			42°		
Mutant	gro$^+$	gro87	gro89	gro+	gro87	gro89	gro+	gro87	gro89
WT	1.0	10^{-7}	10^{-4}						
ogr(rep)-F G88V	1.0	10^{-2}	1.0	0.6	10^{-2}	0.5	10^{-4}	10^{-4}	10^{-4}
ogr(rep)-F P174R	1.0	10^{-5}	1.0	1.0	10^{-5}	1.0	10^{-5}	10^{-5}	10^{-5}
ogr(rep)-F S221L	0.9	10^{-4}	1.0	10^{-2}	10^{-4}	1.0	10^{-4}	10^{-4}	10^{-4}
ogr(rep)-F S227P	0.3	10^{-5}	1.0	0.4	10^{-5}	0.6	10^{-4}	10^{-5}	0.5
ogr(rep)-F A346V	1.0	10^{-4}	0.1	10^{-2}	10^{-4}	0.5	10^{-5}	10^{-4}	10^{-5}
ogr(rep)-F P417S	1.0	10^{-4}	0.5	0.3	10^{-4}	0.3	10^{-4}	10^{-4}	10^{-4}
ogr(rep)-A A80P	0.5	1.0	0.5				0.1	10^{-2}	10^{-5}
ogr(rep)-A D82G	0.3	10^{-4}	1.0				0.3	10^{-5}	0.7
ogr(rep)-A S59F	0.6	10^{-5}	1.0						
ogr(rep)-A/A S59F/D82G	0.4	0.4	1.0						
ogr(rep)-A/F D82G/P417S	0.4	1.0	0.9						
ogr(rep)-A/F A80V/P417S	1.0	0.9	0.8						
ogr(rep)-A/F A80V/S227P	1.0	0.6	0.9						
ogr(rep)-A/F A80V/S221L	0.5	1.0	0.4						

Efficiency of plating compared assay titer with most permissive titer.

TABLE 3

Burst sizes of *ogr(rep)* mutants in single and coinfections with wild-type ϕX174

Infection/coinfection	Host cell		Progeny ratio[a] *ogr*:wt	
	gro$^+$	gro89	gro$^+$	gro89
WT	143	0.1		
ogr(rep)-F P174R	6.9	42		
ogr(rep)-F P174R XWT	18	46	2:3	3:1
ogr(rep)-F S221L	170	2.3		
ogr(rep)-F S221L X WT	89	19		
ogr(rep)-F S227P	12	2.7	4:5	3:1
ogr(rep)-F S227P X WT	88	4.0		
ogr(rep)-F A346V	380	9.1		
ogr(rep)-F A346V X WT	130	9.7		
ogr(rep)-F P417S	140	16		
ogr(rep)-F P417S X WT	310	18		
ogr(rep)-A A80P	25	280	2:5	44:1
ogr(rep)-A A80P X WT	44	113		

Moi of 10. In coinfections the moi of each infecting phage was 5.0. Burst sizes are ϕ/cell.

[a] Progeny ratios were determined by assaying progeny to grow on the gro$^+$ and gro89 hosts. These ratios were determined by assaying $\geq$45 progeny.

rated by oligonucleotide mediated mutagenesis. The mutagenic primers were designed to restore the wild-type sequence in codons 59 and 82. The mutagenized progeny were screened for phenotypes differing from the *ogr(rep)-A/A S59F/D82G* parent. In both instances, progeny that could only grow in the gro89 host were recovered. DNA was isolated and sequenced in gene *A*. The sequence analysis revealed that the nonparental phage were single *ogr(rep)*-A S59Fand *ogr(rep)*-A *D82G* mutants. To investigate the possibility of interacting mutations in genes *A* and *F*, *A/F* double mutants were selected by plating ogr(*rep*)-*F S221L*, *S227P* and *P417S* mutants on the gro87 host. Regardless of the parental *ogr(rep)-F* mutant used, the second mutations were always located in gene *A* and conferred amino acid substitutions at the common positions of 80 or 82. These results suggest that at least these *A/F* interactions are not allele specific (Table 2).

To obtain a more quantitative measure of *ogr(rep)-F* mutant growth, burst sizes were assayed in the gro89 and gro$^+$ hosts. The results of these experiments are in Table 3. The *ogr(rep)-F* infections yielded bursts ranging from 2.3–46 ϕ/cell in the gro89 host. These burst sizes reflect titers that were at least fivefold higher than the titer of unabsorbed phage, determined as described in MATERIALS AND METHODS. These results indicate that the *ogr(rep)* mutations raise burst sizes to a level consistent with the conditions under which the mutants were isolated. The wild-type ϕX 174 infection, on the other hand, produced a burst of 0.1 ϕ/cell, which was equal to the titer of unabsorbed virions. The burst sizes of coinfected cells were also determined. The bursts produced were equal to those produced in *ogr(rep)* single infections, indicating that the *ogr(rep)* phenotype is dominant.

TESSMAN and PETERSON (1976) reported that an S13 *ogr* mutation in gene *F* conferred a *cis* dominant phenotype. S13 and ϕX 174 are very closely related with ~98 and 98.5% homology on the DNA and protein level, respectively (LAU and SPENCER 1985). They reported a ratio of progeny phage from coinfected gro89 infected cells (*ogr:non-ogr*) of ~12:1. The *non-ogr* parents were various S13 amber mutants. A much smaller *cis* dominant effect, which may not be significant, was observed in the experiments reported in Table 3. The ratio of recovery (*ogr*:wt) was skewed toward *ogr(rep)-F* progeny when gro89 was the infected host. Conversely, the ratio of recovery was skewed toward wt progeny in gro$^+$ infected cells. These ratios were determined by plating the progeny on the mutually permissive gro$^+$ host. Progeny plaques were then stabbed into gro89 and gro$^+$ indicator lawns. This slight *cis* dominant effect, however, was dramatically lower than that observed from the *ogr(rep)-A* × wt coinfection (44:1). The *cis* acting nature of the gene *A* protein has been well documented (FRANCKE and RAY 1971b; EISENBERG and KORNBERG 1979).

Three factors may account for the differences between the two data sets. First, the use of amber mutants as the *non-ogr* parent in the experiments of TESSMAN and PETERSON (1976) may have skewed the recovery toward *ogr* progeny. Second, the S13 coat protein may indeed be *cis*-acting while the ϕX 174 coat protein is not. And finally, it is possible that the mutant used in the studies of TESSMAN and PETERSON was an *A/F* double mutant. Like the *ogr(rep)-F* mutants described in this report, it had a secondary *ts* phenotype that was used to map the mutation to gene *F* by complementation. The nucleotide sequences of ϕX 174 and S13, however, were unknown in 1976; hence a DNA sequence analysis could not have been conducted. Unlike the *ogr(rep)-F* mutants described in this report, the mutant isolated by TESSMAN and PETERSON (1976) propagated on the gro87 host. The ability to propagate on the gro87 host is consistent with the phenotype of the *ogr(rep)-A* and *ogr(rep)-A/F* double mutants reported here.

DISCUSSION

The mutant gro89 rep protein blocks the formation of the 50S complex: Stage III DNA synthesis and packaging occurs exclusively in the 50S complex assembly intermediate of which the viral prohead is a component (MUKAI *et al.* 1979). The 50S complex is formed by the association of the viral prohead with the DNA preinitiation complex, consisting of RF II DNA, gpA, gpC and the host cell *rep* protein (AOYAMA *et al.* 1983). TESSMAN and PETERSON (1976) isolated *rep* mutants that specifi-

cally block stage III DNA synthesis. In deproteinized samples, no single-stranded DNA was detected in infected *rep* mutant cells. The formation of the 50S complex, however, was not examined.

As discussed in the Introduction, there are several blocks in the assembly pathway that could result in the absence of single-stranded DNA synthesis. To distinguish between these possibilities, radio-labeled extracts (^{3}H-protein or ^{3}H-DNA) were prepared from gro89 and gro$^+$ (wild-type) infected cells and analyzed by sucrose gradient sedimentation. The results of these experiments suggest that the 50S complex cannot form in gro89 infected cells. The mutant *rep* proteins, however, do not interfere with the formation of the viral prohead or block earlier stages of DNA replication as reported by TESSMAN and PETERSON (1976). A similar analysis was also conducted with radio-labeled protein extracts prepared from gro87 cells (data not shown). In these extracts, a particle that sediments at 50S was observed. It was, however, present in reduced amounts when compared to the gro$^+$ extract. As evinced by the *ogr(rep)-A A80P* mutation, which restores growth in both of the gro89 and gro87 hosts, the defects conferred by the mutant *rep* proteins are related. The gro87 *rep* protein may inhibit, but not prohibit, 50S complex formation. The 50S complexes that do form, however, are most likely not functional.

Two models could account for the lack of 50S complex formation and/or stabilization in the gro89 host. If the mutant *rep* proteins cannot associate with the other components of the preinitiation complex, the 50S complex would not form. AOYAMA *et al.* (1983) demonstrated that 50S complex formation is blocked if any component of the RF II-gpA-*rep*-gpC preinitiation complex is not present. Alternatively, the preinitiation complex may form but be unable to associate with the viral prohead. Genetic data argue for the second alternative. Preinitiation complex formation does not require the F protein (AOYAMA *et al.* 1983). Because single mutations in gene *F* are enough to confer a viable phenotype in the gro89 host, the gro89 *rep* protein most likely does not interfere with preinitiation complex formation. This hypothesis, however, will need to be tested further.

Characterization of *ogr(rep)* mutants: Two distinct *ogr(rep)* phenotypes were apparent among the selected mutants, *ts* and *ts*$^+$. All of the *ts ogr(rep)* mutations were located in gene *F*. The *ts*$^+$ *ogr(rep)* mutations, on the other hand, were found in gene *A*. The *ogr(rep)* mutants do not propagate in cells carrying a putative null allele of the *rep* gene and the allele specificty of the *ogr(rep)-F* mutants indicate that the *ogr(rep)* mutations do not confer the ability to propagate independently of *rep* protein function. The bursts produced in wild-type × *ogr(rep)-F* co-infections indicate that the *ogr(rep)* phenotype is dominant. Although this suggests that hybrid proheads are capable of 50S complex formation and DNA packaging, a model in which the two different coat proteins independently assemble into homogenous proheads cannot be ruled out. Regardless of the model, the dominant phenotype is not surprising. If the two coat proteins do not associate, homogenous *ogr(rep)-F* proheads would be present and phage would be produced. In a hybrid prohead model, only a limited number of *ogr(rep)-F* coat proteins need be present as long as they form a productive association site for the preinitiation complex.

The location of the *ogr(rep)-F* mutations in the atomic structure of the virion: Two previous second-site genetic analyses have laid the foundation of a rudimentary structure/function map of the ϕX 174 coat protein (FANE and HAYASHI 1991; FANE *et al.* 1993). These analyses identified assembly sequences that influence the formation of the 12S particle, and secondary structures that influence the stabilization of the viral prohead (EKECHUKWU and FANE 1995). A schematic of the major coat protein is presented in Figure 3. Analyses of atomic structures and dissociation studies conducted with a wide variety of virions led to the hypothesis that these loops, as opposed to the beta-barrel core, may play a crucial role in viral assembly (KIM *et al.* 1990; LIDDINGTON *et al.* 1991; MCKENNA *et al.* 1992). As observed with the other assembly mutations, all of the *ogr(rep)-F* mutations are located in the loops of the atomic structure. This is consistent with the hypothesis that assembly interactions are mediated by the amino acid loops of icosahedral coat proteins.

The locations of these various mutations may also provide insights into the functions of various structures found in the major coat protein. The *suD* mutations, for example, are located in α-helical regions that are found near the threefold axis of symmetry in the folded protein. The *ogr(rep)-F* mutations, on the other hand, are localized near the twofold axis of symmetry and have access to the surface of the virion. Four of these mutations map to a striking depression which skirts the twofold axis of symmetry.

50S complex formation/stabilization, general considerations and mechanisms: Unlike tailed bacteriophage, Microviridae capsids do not contain a unique vertex for translocating DNA into the prohead. The structure of the ϕX 174 prohead, as determined by cryoelectron microscopy reconstruction (ILAG *et al.* 1995), reveals large pores at the threefold axis of symmetry in each face of the icosahedral. No such pores exist at the fivefold axis. Packaging, as ILAG *et al.* suggest, may occur through a face of the prohead, not a vertex. If the virus is to efficiently propagate, conformational changes must occur in the prohead upon the formation of the 50S complex to ensure that packaging proceeds at only one location.

The data presented here support two alternative models of 50S complex formation or stabilization. Because many substitutions in gpF can restore the ability to propagate in gro89 cells, it is unlikely that these

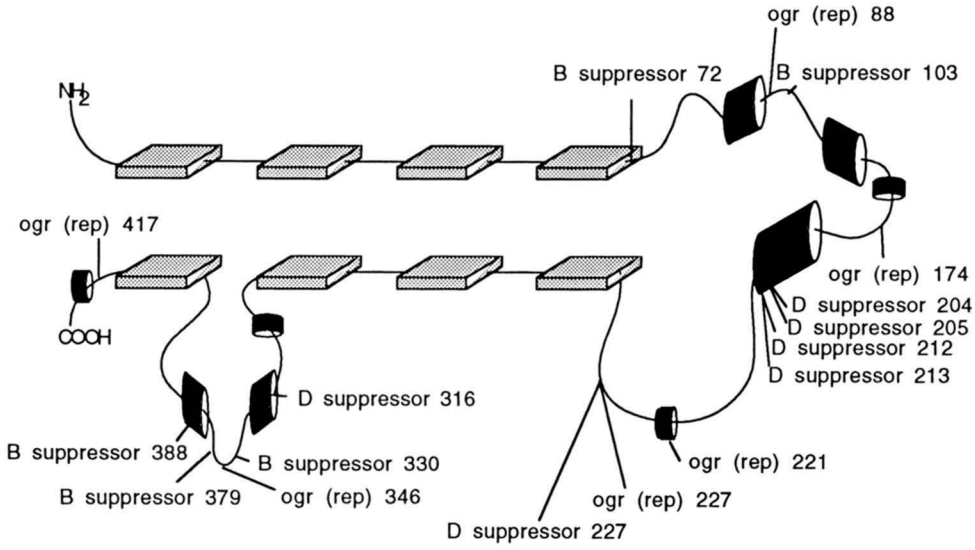

FIGURE 3.—Schematic map of the ϕX 174 coat protein. Elongated boxes represent the β-sheets comprising the β-barrel. Cylinders depict α-helices. Substitutions are denoted by genotype. The *B suppressors* affect the formation of the 12S particle; the *D suppressors* affect the stability of the prohead (FANE and HAYASHI 1991; FANE *et al.* 1993; EKECHUKWU and FANE 1995). The *ogr(rep)* mutations are described in this report.

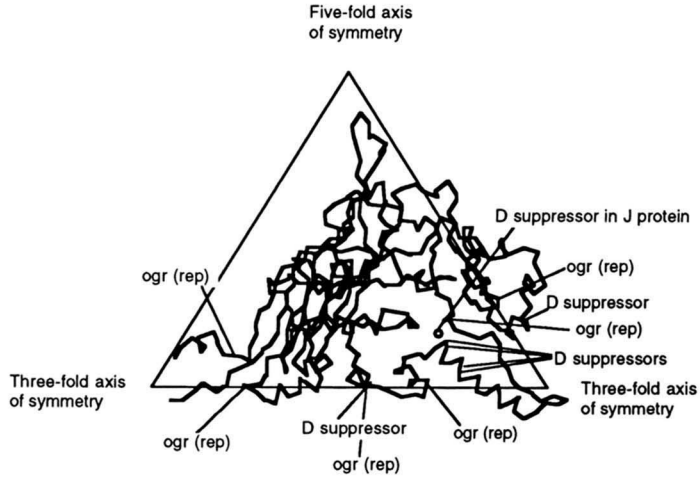

substitutions are all in contact with the mutated amino acid in the gro89 *rep* protein. The mechanism of suppression is most likely general. The amino acid sites identified by the *ogr(rep)-F* mutations, or the depression along the twofold axis of symmetry in which the majority of them are located, may be crucial to mediating conformational changes in the prohead upon binding of the preinitiation complex. In this model, the mutant preinitiation complexes would be unable to trigger the conformational changes necessary for 50S complex stabilization. In turn, the *ogr(rep)-F* mutations would restore the ability to achieve the required conformational changes and subsequent stability. Because the *ogr(rep)-F* mutations confer a dominant phenotype, it follows that only a subset of the coat proteins need be the *ogr(rep)-F* species. Alternatively, the *ogr(rep)-F* mutations, or the depression along the twofold axis of symmetry, may identify the actual contact site between the preinitiation complex and prohead during 50S complex formation. Structural rearrangements along the twofold axis or in the preinitiation complex, via mutations in gpA, may facilitate this association in the gro89 infected cells. This model is also consistent with the observed dominant phenotype of the *ogr(rep)-F* mutations, because binding and packaging would occur at only one site in the particle.

The authors thank H. WOOD for editorial assistance, Drs. R. MCKENNA and M. ROSSMANN for discussion, and Dr. MASAKI HAYASHI for cell strains and many other valuable gifts. This work was supported by a National Science Foundation/Experimental Program to Stimulate Competitive Research (EPSCOR) grant to the Center for Protein Dynamics at the University of Arkansas. M.C.E. was supported in part by a grant from the Arkansas Science and B.A.F. by a Technology Association grant (ASTA-94B-06)

LITERATURE CITED

AOYAMA, A., and M. HAYASHI, 1986 Synthesis of bacteriophage ϕX 174 *in vitro*: Mechanism of switch from DNA replication to DNA packaging. Cell **47:** 99–106.

AOYAMA, A., R. H. HAMATAKE and M. HAYASHI, 1983 In vitro synthesis of bacteriophage ϕX 174 by purified components. Proc. Natl. Acad. Sci. USA **80:** 4195–4199.

DENHARDT, D. T., D. H. DRESSLER and A. HATHAWAY, 1967 The

abortive replication of ϕX 174 DNA in a recombination deficient mutant of E. coli. Proc. Natl. Acad. Sci. USA **57:** 813–820.

EISENBERG, S., and A. KORNBERG, 1979 Purification and characterization of ϕX 174 gene A protein: a multifunctional enzyme of duplex DNA replication. J. Biol. Chem. **254:** 5328–5332.

EKECHUKWU, M. C., and B. A. FANE, 1995 Characterization of the morphogenetic defects conferred by cold-sensitive prohead accessory and scaffolding proteins of ϕX 174. J. Bact. **177:** 829–830.

FANE, B. A., and M. HAYASHI, 1991 Second-site suppressors of a cold-sensitive prohead accessory protein of bacteriophage ϕX 174. Genetics **128:** 663–671.

FANE, B. A., S. HEAD and M. HAYASHI, 1992 The functional relationship between the J proteins of bacteriophages ϕX 174 and G4 during phage morphogenesis. J. Bact. **174:** 2717–2719.

FANE, B. A., S. SHIEN and M. HAYASHI, 1993 Second-site suppressors of a cold sensitive external scaffolding protein of bacteriophage ϕX 174. Genetics **134:** 1003–1011.

FRANCKE, B., and D. S. RAY, 1971a Formation of the replicative form DNA of bacteriophage ϕX 174 and initial events in its replication. J. Mol. Biol. **61:** 565–586.

FRANCKE, B., and D. S. RAY, 1971b Cis-limited action of the gene A product of bacteriophage. Proc. Natl. Acad. Sci. USA **69:** 475–479

FUJISAWA, H., and M. HAYASHI, 1976 Viral DNA- synthesizing intermediate complex isolated during assembly of bacteriophage ϕX 174. J. Virol. **19:** 409–415.

HAYASHI, M., A. AOYAMA , D. L. RICHARDSON and M. N. HAYASHI, 1988 Biology of the bacteriophage ϕX 174, pp. 1–71 in *The Bacteriophages*, Vol. 2, edited by R. CALENDAR. Plenum Publishing Corporation, New York.

ILAG, L. L., N. H. OLSON, T. DOKLAND, C. L. MUSIC, R. H. CHENG *et al.*, 1995 DNA packaging Intermediates of bacteriophage ϕX 174. Structure **3:** 353–363.

KIM, S., U. BOEGE, S. KRISHNASWAMY, I. MINOR, T. J. SMITH *et al.*, 1990 Conformational variability of a picornavirus capsid: pH-dependent structural changes of Mengo virus related to its host receptor attachment site and disassembly. Virology **175:** 176–190.

LAU, P. C. K., and J. H. SPENCER, 1985 Nucleotide sequence and genome organization of bacteriophage S13 DNA. Gene **40:** 273–284.

LIDDINGTON, R. C., Y. YAN, J. MOULAI, R. SAHLI, T. L. BENJAMIN *et al.*, 1991 Structure of simian virus 40 at 3.8 Å resolution. Nature **354:** 278–284.

MCKENNA, R., L. L. ILAG and M. G. ROSSMANN, 1994 Analysis of the single-stranded DNA bacteriophage ϕX 174 at a resolution of 3.0 A. J. Mol. Biol. **237:** 517–543.

MCKENNA, R., D. XIA, P. WILLINGMANN, L. L. ILAG, S. KRISHNASWAMY *et al.*, 1992 Atomic structure of single-stranded DNA bacteriophage ϕX 174 and its functional implications. Nature **355:** 137–143.

MUKAI, R., R. K. HAMATAKE and M. HAYASHI, 1979 Isolation of the bacteriophage ϕX 174 prohead. Proc. Natl. Acad. Sci. USA **76:** 4877–4881.

SANGER, F., A. R. COULSON, C. T. FRIEDMANN, G. M. AIR, B. G. BARRELL *et al.*, 1978 The nucleotide sequence of bacteriophage ϕX 174. J. Mol. Biol. **125:** 225–246.

TESSMAN, E. S., and P. K. PETERSON, 1976 Bacterial *rep*$^-$ mutations that block development of small DNA bacteriophages late in infection. J. Virol. **20:** 400–412.

Communicating editor: R. MAURER